21

Fabrication of SiC-based Ceramic Microstructures from Preceramic Polymers with Sacrificial Templates and Softlithography Techniques

Tae-Ho Yoon[1], Lan-Young Hong[1] and Dong-Pyo Kim[1,2]
[1]Center of Applied Microfluidic Chemistry, Chungnam National University
[2]Graduate School of Analytical Science and Technology, Chungnam National University
Korea

1. Introduction

Silicon derived polymers containing nitrogen, carbon and boron have been considered as precursors for various non-oxide ceramics such as SiC, SiCN and SiBCN (Madou, 2002, Nguyen & Wereley, 2002, Liew et al., 2003). These ceramics can be easily shaped using various forming processes and then crosslinked by exposure to heat or UV radiation to form an infusible solid. The consolidated preceramic polymers are finally pyrolyzed at high temperatures to transform into the dense ceramic phases. These materials can be used for high temperature applications in areas such as structural composites (Kim et al., 1996), electronic devices (Xia & Whitesides, 1998) and catalytic chemical reactions (Xia et al., 1999). Table 1 shows some selected important preceramic polymers that have been studied in various aspects. In particular, silicon carbide (SiC) is a typical non-oxide ceramic that has attracted the most interest on account of its unique physical and chemical properties such as high thermal conductivity, excellent thermal stability, superior stability towards oxidation compared with carbon, high mechanical strength and chemical inertness. Commercially available polysilazane (VL-20, KiON Corp. USA) and two types of polycarbosilanes, Polymethylsilane (PMS) and Allyhydridopolycarbosilane (Starfire System, USA) are readily used as preceramic polymers for SiCN and SiC ceramics, respectively.

Preceramic polymers	Polymeric unit	Ceramic	Ceramic yield (%)
Polycarbosilane	$(-R_2SiCH_2-)_n$	SiC	65
Polysiloxane	$(-R_2SiO-)_n$	Si-O-C	30-60
Polysilazane	$(-R_2SiNR-)_n$	Si_3N_4	20-90
Aluminum amide	$(=AlNR-)_n$	AlN	20-50
Polyborazine	$(-B_3N_3H_x-)_n$	BN	85
Polytitanium imide	$(=Ti(NR)_2-)_n$	TiN	50-70

Table 1. A list of typical preceramic polymers

Source: Lithography, Book edited by: Michael Wang,
ISBN 978-953-307-064-3, pp. 656, February 2010, INTECH, Croatia, downloaded from SCIYO.COM

A variety of synthetic approaches have been proposed for the development of porous materials with a high surface area and a controlled pore size distribution due to their many potential applications. There are many reports on the variety of porous carbon, oxides, sulfides and metals prepared from various hard and soft templates. Moreover, porous ceramics with a different porous morphology and size distribution have been fabricated via different routes, such as burning out a polymeric sponge impregnated with a solid-state sintering (Kwon et al., 1994), replica of a polymer foam by impregnation (Peng et al., 2000), ceramic slurry (Zhu et al., 2002), sol-gel process (Geis et al., 2002) and gel casting methods (Zhang et al., 2006). Because of the low oxidation resistance of carbon and the poor hydrothermal stability of porous silica materials, SiC with a high surface area has attracted considerable attention as a support material in the catalysis. Therefore, several attempts have been made to prepare various SiC macroporous and mesoporous materials.

On the other hand, the fabrication of 3D microstructures has been recently developed for use in photonic crystals, biochips, micro/nanofluidic devices and nano/micro-electromechanical systems (N/MEMS) (Yamazaki & Namatsu, 2004, Lee & Seung, 2004). In addition, it is expected that there will be considerable demand for ceramic devices that can be used in harsh environments in the fields of aerospace, military and energy industry. In terms of practical fabrication techniques, the mechanical method of machining has mainly been used for various materials and has played an important role in the fabrication of ceramic microstructures. However, this method has shortcomings when it comes to fabricating controlled 3D ceramic microstructures. As an alternative to the machining process, lithographic techniques have been investigated for producing 3D ceramic microstructures with a nanoscale resolution using preceramic polymers or ceramic-powder mixed polymers.

This chapter reviews the recent development of porous SiC materials from templated preceramic polymers and the fabrication of small and complicated SiC ceramic features using near-net shape processing techniques such as soft lithography. There is a need to summarize these types of SiC structural materials on the nanoscale in order to extend their utility into nanotechnology devices. Besides, it is obvious that one of the challenging strategies in ceramic applications is the integration of preceramic polymers into existing manufacturing processes to achieve nano-level process control and the ability to produce useful architectures. In this context, it is meaningful to introduce several preliminary results from our own laboratory in this area.

2. Porous ceramic structure form sacrificial template

This section defines the scope for the preparation of various SiC porous materials using different types of sacrificial hard templates. The main concern is on macroporous SiC with pores larger than 50 nm, mesoporous SiC with pores ranging from 2 to 50 nm, and SiC nanotubes. These porous ceramics have a wide variety of applications including filters, membranes, sensors, catalyst supports, as well as biomedical and construction materials (Sepulveda, 1997).

2.1 Macroporous SiC-based ceramics

There have been many studies on macroporous structures using oxide and carbon materials, but there are only few on SiC for making macroporous structures. The macroporous structure has the advantage of a lower pressure drop than that of a mesoporous structure

when used as a catalyst support. Table 2 shows the various precursors and templates used to prepare macroporous SiC and SiCN ceramic materials. According to the Quin et al., a SiC based macropore structure 'wood ceramic' was prepared from carbonized wood powder and phenol resin via a direct reaction with Si powder (Quin, 2003). But, the wood ceramic product showed disordered porosity with broad range of pore size distribution. Accordingly, the sacrificial template method has been used in the manufacture of highly ordered macroporous materials with a narrow pore size distribution. Firstly, homogeneous colloidal silica spheres ranging in size from 137 to 700 nm, as shown in figure 1(a) and (b), were gently precipitated to form a closed packed crystal template (Sung et al., 2002). A low molecular weight polymer precursor, polymethylsilane (PMS), was then infiltrated into the sacrificial colloidal silica crystalline arrays, which were subsequently etched with HF after pyrolysis in an argon atmosphere (Wang et al., 2004). Pore sizes of approximately 84~658 nm and a BET surface of approximately 585 m^2g^{-1} ~ 300 m^2g^{-1} of the obtained porous products in proportion to the sizes of the sacrificial templates were obtained. It is believed that the high surface area was due to the interfacial area between the sphere and the infiltrated polymer as well as to the formation of micropores at the ceramic wall during pyrolysis. In addition, 3-dimensionally ordered macroporous (3DOM) SiC ceramics were prepared using polysilazane and silica spheres ranging in size from 112 to 650 nm. This was followed by a thermal curing step, pyrolysis at 1250 °C in a N_2 atmosphere, and an identical etching process (Wang et al., 2005). Table 3 summarizes the comparative pore characteristics using silica sphere templates with various sizes (112 ~ 500 nm) and different types of preceramic polymers.

On the other hand, porous carbon was used as an alternative sacrificial template to prepare a different type of macroporous SiC ceramic with a unique morphology. A 3DOM carbon template was prepared by infiltrating sugar or phenolic resin into a closed packed silica

Precursor	Template	Final product	Pore sizes and types	BET surface area (m^2g^{-1})	Ref.
phenol resin, Si	wood powder	SiC	10-30㎛ Irregular channel	--	Quin et al., 2003
PMS PCS	monolayered silica sphere (500nm)	SiC	340 nm ordered macropore	150~172	Sung et al., 2002
PMS, polysilazane	macroporous carbon (150-1000 nm)	SiC SiCN	135-896 nm hollow spheres	50.8-5.0	Wang et al., 2004
PMS, PCS PMS&PCS hybrid	alumina membrane (100-400 nm)	SiC	200 nm hollowed tube	339	Wang et al., 2005
polysilazane	silica spheres (112-650 nm)	SiCN	98-578 nm ordered macropore	455.6-250.3	Wang et al., 2005

Table 2. Summarized characteristics of the macropores originating from different precursors and templates.
PMS: polymethylsilane, PCS: polycarbosilane

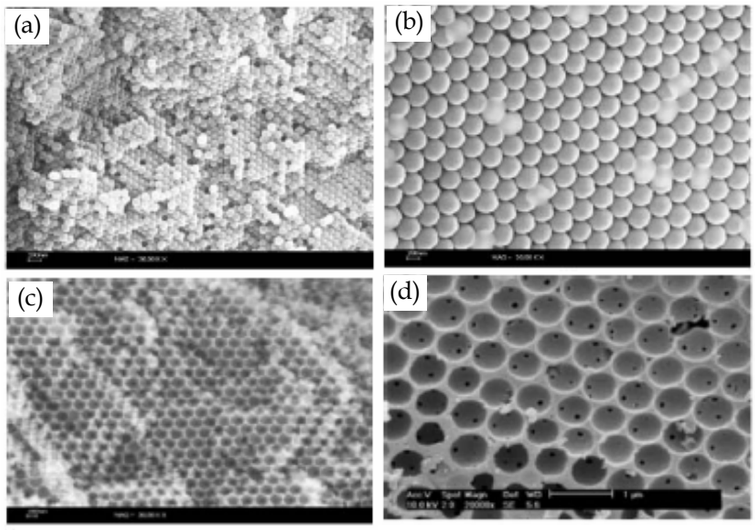

Fig. 1. The SEM images of a representative silica template and porous SiC with different diameters; (a) 137 nm silica template (b) 300 nm silica template, (c) porous SiC from 192 nm template and (d) Porous SiC from 700 nm silica template (Sung et al., 2002).

Precursor	SiO_2 sphere (nm)	BET Surface area ($m^2\ g^{-1}$)	Average pore size (nm)	Pore volume ($cm^3\ g^{-1}$)	Ref.
SiC	112	584.6	4.9	0.68	Wang et al., 2004
	300	387.1	4.9	0.35	
	500	362.3	2.8	0.26	
SiCN	112	455.6	4.5	0.31	Wang et al., 2005
	243	367.7	3.8	0.23	
	500	316.4	3.1	0.18	
BCN	145	412.9	2.5	0.40	Hong et al., 2005
	300	387.1	2.4	0.35	
	500	315.3	4.9	0.27	
SiBCN	145	220.5	2.5	0.14	Hong et al., 2005
	300	211.7	3.9	0.12	
	500	203.2	5.0	0.11	
SiC-$MoSi_2$	500	232.4	3-5	0.46	Wang et al., 2005

Table 3. Summarized pore characteristics of various ordered macroporous ceramics obtained from silica sphere templates and different preceramic polymers.

sphere assembly, followed by an oxidation or curing step and subsequent carbonization at 900 °C (Wang et al., 2004). The 3DOM carbon, as a sacrificial template, was gently infiltrated by low molecular weight preceramic polymers. In order to obtain the hollow nanosphere assembly, a polymeric precursor diluted to 25 mass% in THF was used to induce polymer adsorption on the inner wall of the carbon template during solvent evaporation. The carbon-precursor composites were cured at 160 °C for 6 hr, and then pyrolyzed at 1250 °C. Finally,

the carbon was oxidized at 650 °C in air to obtain an interconnected SiC sphere assembly, as shown in figure 2(a). The TEM image (figure 2(b)) clearly shows a regular ordered array of hollow spheres with dense shells (Wang et al., 2005). It should be noted that a hollow nanosphere with an empty core and inter-connections might have applications as capsules for drug delivery systems (DDS), pigment stabilizers in paints, photonic materials, chemical and biological sensors, and catalysts (Caruso etal., 2001). On the other hand, an ordered assembly of SiCN ceramic spheres with filled cores was produced when low viscous polysilazane with no dilution was inserted into a carbon template, as shown in the SEM and TEM image in figure 2(c) and (d), respectively. The filled SiCN sphere nanostructures with diameters ranging from 142 to 944 nm were proportional to the initial pore sizes of the sacrificial carbon templates used (approx. 150 ~ 1000 nm).

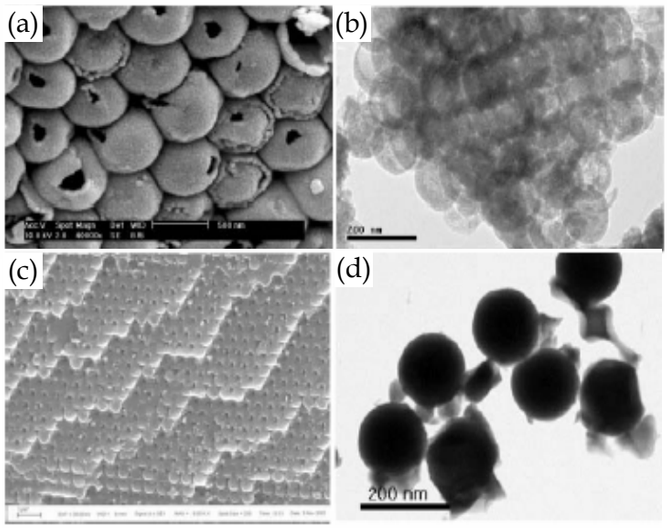

Fig. 2. Three representative SEM(a) and TEM(b) images of 500nm and 135nm hollow SiC sphere assemblies, and SEM(c) and TEM(d) images of 613nm and 142nm filled SiCN sphere assemblies, respectively (Wang et al., 2005).

2.2 Mesoporous SiC-based ceramics

Since mesoporous silicates (M41S) were first discovered in the early 1990s, many efforts have been devoted to producing various mesostructure materials including mesoporous carbon CMK-I, oxides and metal. The use of a hard sacrificial template for the replication of nanoscale structures using a direct-templating process has sparked excellent contributions in this field. According to this strategy, some disordered mesoporous SiC materials were originally prepared using gas-phase infiltration techniques. For example, Pham-Huu et al. prepared high surface area SiC by a reaction between SiO vapor and active charcoal at temperatures ranging from 1200 to 1500 ^{o}C, which is known as the shape-memory synthesis (SMS) method (Pham-Huu et al., 1999). Parmentier et al. synthesized mesoporous SiC with a surface area of 120 m^2g^{-1} via a carbothermal reduction reaction between mesoporous MCM-48 silica with pyrolytic carbon filled using chemical vapor infiltration (CVI) with propylene as the carbon precursor at temperatures ranging from 1250 to 1450 ^{o}C (Parmentier et al., 2002). Krawiec et al. produced disordered mesoporous SiC with a high surface area (508 m^2g^{-1}) using a CVI process involving the introduction of a gaseous SiC precursor,

dimethyldichlorosilane (DDS), into nanoporous SBA-15 silica as summarized in Table 4 (Krawiec et al., 2004).

Template	Structure	SiC precursor	Space group	S_{BET}(m^2g^{-1})
Active Charcoal	Disordered	SiO vapor, Carbon	-	~100
MCM-48	Disordered	C, SiO_2	-	120
SBA-15	Disordered	DDS vapor	-	508
Silica nanosphere	Disordered	AHPCS	-	612
SBA-15	Ordered	AHPCS	*P6mm*	260
MCF	Ordered	AHPCS	Unknown	250
SBA-15	Ordered	PCS	*P6mm*	720
KIT-6	Ordered	PCS	*Ia3d*	590

Table 4. Comparative summary of the reported mesoporous SiC products and corresponding templates.

The first report on the production of mesoporous SiC using a preceramic polymer showed a simple method, similar to that used to produce macroporous SiC, involving the infiltration of low viscous allyhydridopolycarbosilane (AHPCS, SP matrix, Starfire sys., USA) into a randomly packed silica colloidal sphere template with a diameter of 20 ~ 30 nm. The disordered mesoporous SiC exhibited an amorphous foam-like SiC with a high surface area of 612 m^2g^{-1} and a total pore volume of 0.81 cm^3g^{-1} (Park et al., 2004). The above mesoporous SiC showed no long-range order of porosity because the silica nanosphere could not be precipitated into a closed-packed mode as a result of the strong electrostatic interactions between spheres. Because ordered mesoporous carbon such as CMK-3 have been formed from the use of ordered mesoporous silica templates, highly ordered mesoporous SiC materials were also prepared using trimethylsilyated SBA-15 and mesocellular siliceous foam as sacrificial hard templates. It is well known that SBA-15, which is prepared using triblock copolymers as a structure directing agent, is a two-dimensional hexagonally ordered mesoporous silica with channel-interconnecting micropores (6.5 nm) within the wall (Zhao et al., 1998). Mesocellular siliceous foam was also composed of uniform and large spherical cells (~20 nm) and connecting windows (Schmidt-Winkel et al., 1999). The diluted allylhydridopolycarbosilane was infiltrated into two types of surface modified nanoporous silica templates. The silica templates were subsequently etched off after pyrolysis at 1000 ^oC under a nitrogen atmosphere to leave an ordered mesoporous structure. Both synthesized mesoporous SiC materials had a high BET surface area in the range of 250~260 m^2g^{-1} with a pore size of 3.4~3.6 nm. The mesoporous SiC materials prepared from the two types of silica templates were exact inverse replicas of their templates, as shown in figure 3 (Yan et al., 2006).

A similar study was also carried out by Zhao's group as listed in Table 4. Highly ordered mesoporous SiC ceramics were synthesized via a one-step nanocasting process using commercial polycarbosilane (PCS) as a precursor and mesoporous silica materials, SBA-15 and KIT-6, as hard templates (Shi et al., 2006). The obtained mesoporous SiC ceramics with 12% excess of carbon were amorphous below 1200 °C, and were composed of randomly oriented β-SiC crystallites after being heated to 1400 °C. These ordered mesoporous SiC

ceramics had very high BET specific surface areas up to 720 m^2g^{-1}, large pore volumes (ab. 0.8 cm^3g^{-1}) and a narrow pore-size distribution (2.0~3.7 nm). It is expected that these novel techniques will be suitable for synthesizing many other types of ordered mesoporous non-oxide ceramic materials with interesting pore topologies.

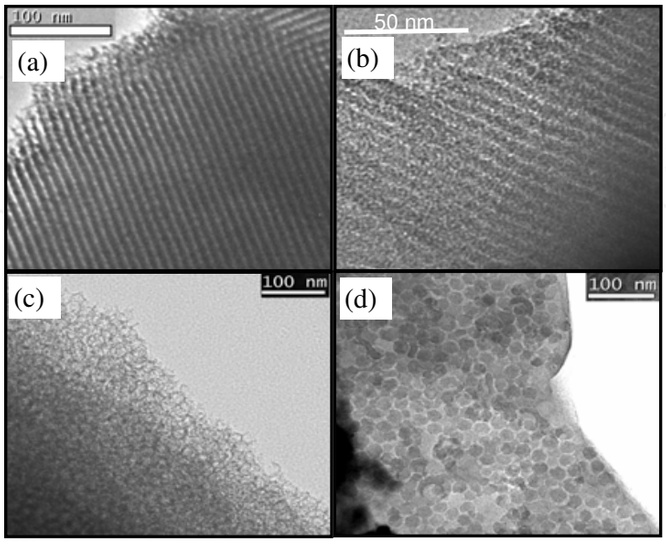

Fig. 3. TEM images of the mesoporous SiC products and corresponding nanoporous silica templates. (a) SBA-15 template, (b) SiC product from SBA-15, (c) MCF template and (d) SiC product from MCF (Zhao et al., 1998).

It should be noted that the porous SiC products prepared from silica templates had severe oxygen contamination as a result of oxygen diffusion at the interface during the pyrolysis of the infiltrated preceramic polymers. The mesoporous SiC obtained had a surface severely contaminated with SiC_xO_y impurities, which is detrimental to high temperature applications. Therefore, it is desirable to use a sacrificial template containing no oxygen, which can avoid the formation of silicon oxycarbide species in the produced mesoporous SiC. In this context, it is deserved to introduce that mesoporous boron nitride (BN) with a specific surface area of 540 m^2g-1, a mesoporous volume of 0.27 cm^3g^{-1}, and a narrow pore size distribution (4.4 nm), was obtained from tri(methylamino)borazine as a precursor using CMK-3 mesoporous carbon as a non-oxygen template (Dibandjo et al., 2005). The mesoporous carbon template route appears to be a promising method for fabricating mesoporous ceramics from polymeric precursors. BN and BCN nanostructures were alternatively prepared via a substitution reaction using carbon templates (Vinu et al., 2005).

2.3 SiC nanotube structure

Since the discovery of carbon nanotubes in 1991, there has been considerable interest in fabricating one-dimensional tubular structures for their potential applications as electric devices and sensors (Iijima, 1991). Recently, many types of organic materials (peptide, polypyrrole) and inorganic materials (nitride, sulfide, oxide, carbide) have been considered in the preparation of tubular structures (Wu et al., 2004). Different types of tubular SiC nanostructures were synthesized since Dai et al. first reported the preparation of SiC nanotubes using a shape memory synthesis method (Dai et al., 1995, Keller et al., 2003). Most preparation methods are based on a carbothermal reduction and/or chemical vapor

deposition, resulting in randomly dispersed nanotube structures. An alumina (Al_2O_3) membrane with a 200 nm diameter was used as a template for making SiC arrays with a well-aligned tubular structure and a tailored diameter and wall thickness. A polymethylsilane solution was infiltrated into the dried alumina membrane at room temperature under a nitrogen atmosphere. After vacuum evaporation, the infiltrated polymer was cured and the polymer was heated to 1250 °C in an argon atmosphere. Figure 4 shows SEM and TEM images of well-aligned array of SiC tubes with a uniform wall thickness 35 nm. The SiC nanotube had an electrical resistance of 6.9 × 103 to 4.85 × 103 Ωm at temperatures ranging from 20 to 300 °K with a negative temperature dependence, which is similar to a semiconductor-like behavior. In addition, Pt/Ru alloy nanoparticles could be selectively deposited on the inner wall of the nanotube. This material might be useful in the fields of heat-resistant nanodevices, fuel cells and nanofluidic devices.

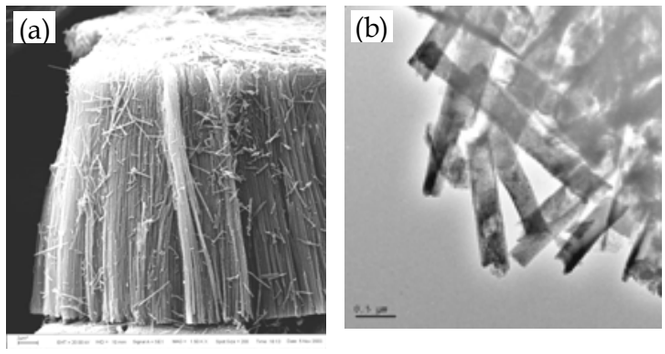

Fig. 4. The representative SEM(a) and TEM(b) image of 100nm tubular SiC derived from PMS (Wang et al., 2005).

3. Ceramic nanostructure via lithographic techniques

Whitesides suggested the use of elastomeric silicone rubber, mainly polydimethylsiloxane (PDMS), for micropattern transfer known as soft lithography (Whitesides et al., 1999). Soft lithography is a valuable tool for the low-cost microstructuring of liquid materials (Heule & Gauckler, 2001, Heule & Gauckler, 2003, Martin & Aksay, 2005). There are several variations available that are suited for the direct patterning of polymeric liquids. Microcontact printing (μ-CP) is used for stamping self-assembled monolayers serving as a resist or as functional layers. Replica molding is an efficient method for duplicating the information (i.e. shape, morphology and structure) present on the surface of a mold. In microtransfer molding (μ-TM), a thin layer of a liquid prepolymer is applied to a patterned surface of a PDMS mold and the excess liquid is removed by scraping it with a flat PDMS block or by blowing it off with a nitrogen stream. A low-viscosity fluid was patterned through the spontaneous filling of PDMS microchannels by capillary action in micromolding in the capillaries (MIMIC) (Heule et al., 2003). After curing the prepolymer into a solid, the PDMS mold was removed to reveal patterned microstructures of the polymer. In the imprinting method, a mold was pressed into a layer of a viscous prepolymer film on a substrate, which can flow under pressure to conform to the mold (Guo et al., 2004, Donsel et al., 2001, Chou et al, 1995).
It should be emphasized that synthetic routes using preceramic polymers are promising for producing small and complicated SiC ceramic features using soft lithography and a

modified version of near-net shape processing techniques. Furthermore, recent developments for fabricating a porous channel structures have been introduced as a preliminary work for ceramic microreactor applications.

3.1 Non-porous ceramic patterning via softlithography

Most currently used MEMS devices in the silicon semiconductor industry are fabricated using photolithography coupled with surface machining and wet etching, which is the most common method for obtaining the micrometer sized surface features needed for sensors and actuators. Recently, the use of preceramic polymers offers a simple route for fabricating 2- or 3-dimensional ceramic microstructures using soft lithography techniques. SiC ceramic line patterns on the micron scale were fabricated using MIMIC method, which involved filling PDMS channels that had been formed by conformal contact of a low viscosity preceramic polymer to a silicon wafer, followed by curing and pyrolysis at 800 °C (Hong & Kim, 2005). Moreover, fine ceramic line patterns were also made by applying PDMS mold transfer techniques. Figure 5 shows SEM images of the dense SiC ceramic line patterns, which were exact replicas of the CD and DVD relief structure as an economic master, respectively (Dat etal., 2006). This suggests that preceramic polymers have excellent patterning processibility even on the nanoscale level by efficiently filling a narrow gap. This preliminary study highlights the feasibility of developing high temperature resistant nanoscale ceramic components including MEMS as well as NEMS (nano electromechanical system).

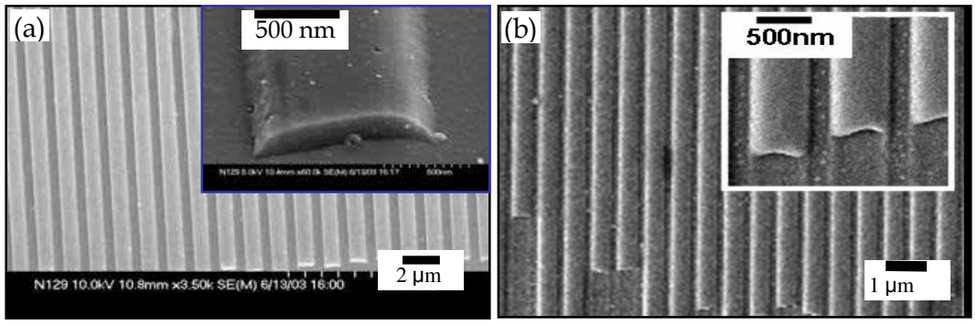

Fig. 5. SEM images of the imprinted SiC ceramic precursor pyrolyzed at 800 oC in an argon atmosphere; (a) SiC line pattern from CD master, (b) SiCN line pattern from DVD master.

R. Raj's group reported the very meaningful achievement by preparing SiCN ceramic MEMS devices using polyureamethylvinylsilazane as a precursor (Liew et al., 2001, Liew etal., 2002, Shah & Raj, 2005). Even primitive types of high-temperature MEMS, i.e. electrostatic actuators, a pressure transducers, and combustion chambers were developed mainly using preceramic polymers that forms SiCN ceramics by pyrolysis via a temperature or radiation induced transformation of a processable liquid state to an infusible solid state (cured polymer). This suggests that multi-layered ceramic MEMS can be fabricated by adding and curing successive layers of liquid polymers on top of each other using multi-level photopolymerization.

3.2 Porous SiC-based ceramic channels for microreactor

This section summarized the preparation of tailored, highly uniform SiC and SiCN porous structures by filling the void space in packed beds of silica spheres with a low viscous preceramic polymer. However, these products are a powdery type, which limits their utility

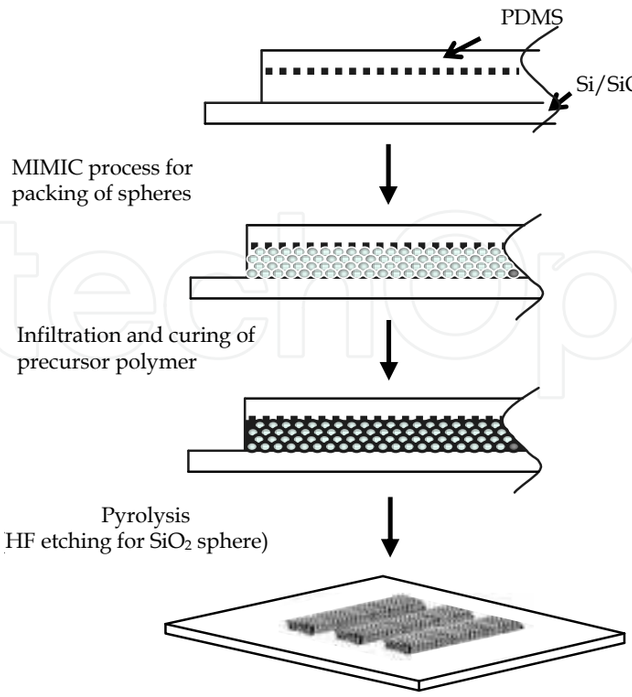

Fig. 6. Schematic diagram of the fabrication steps used to prepare microchannels.

to existing applications. Recently, we reported that the integration of templated preceramic polymers into a new fabrication technique such as soft lithography can produce useful products with new architectures. For the fabrication of tailored porous SiC and SiCN microchannels, as shown in figure 6, a PDMS mold was placed onto the flat surface of a silicon wafer, forming open channels at both ends. A solution containing colloidal silica or polystyrene spheres was allowed to flow slowly into the channels from one and end via capillary forces. The void space between the spheres was filled with the preceramic polymer through capillary action. After curing the preceramic polymer, the colloidal polystyrene spheres were decomposed during the early stages of the pyrolysis process, as shown in figure 7 (Sung et al., 2005). The inverted beaded SiC porous monoliths showed a crack-free ceramic microchannel replica with 150 ~ 200 nm of interconnecting windows for the 1 μm spheres used. The pore size could be tailored independently according to the bead size, allowing for the easy integration of porous monoliths into a microreactor. The SiC ceramic monoliths obtained were used in the decomposition of ammonia after depositing a ruthenium catalyst via wet impregnation and calcinations. The efficient conversion of NH_3

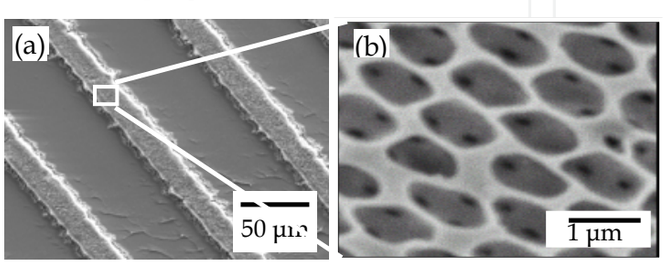

Fig. 7. SEM micrographs of (a) SiCN microchannel replica and (b) its 3-dimensionally interconnected pore structure containing 1 μm pores formed by pyrolysis (Sung et al., 2005).

to H_2 with increasing reaction temperature demonstrated its successful performance as a hydrogen reformer for fuel cells, as shown in figure 8. These novel porous materials show great promises for use in high temperature micro-reactors possibly for the on-demand reforming of higher hydrocarbons into hydrogen for portable power sources.

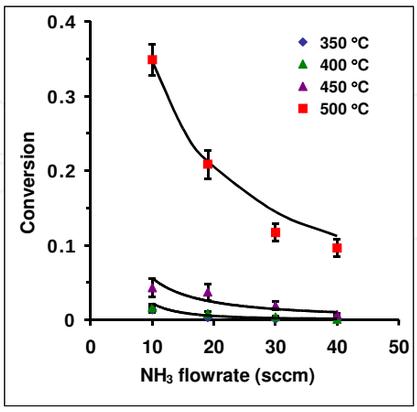

Fig. 8. Ammonia (NH_3) conversion as a function of temperature for different flow rates measured at different temperatures.

4. Advanced ceramic derived microstructure via softlithography

4.1 Fabrication of three-dimensional SiC ceramic microstructures with near-zero shrinkage via dual crosslinking induced stereolithography

3D ceramic microstructures with a submicron resolution will be very useful for a wide variety of applications to ceramic nanodevices. However, the general properties of organic polymers are not sufficient for the devices applicable to harsh environments requiring a tolerance to high temperatures, a resistance to corrosion, as well as tribological properties. Therefore, it is clear that there is a continuous demand for the development of a fabrication process of ceramic structures on the micro- or nano-scale. In terms of feasible fabrication techniques, the mechanical method of machining process has been widely utilized for various materials and has played an important role in fabricating ceramic microstructures. However, this has shortcomings when it comes to the fabrication of arbitrary 3D ceramic microstructures. For the alternative of machining process, the soft lithography and micro-stereolithography have been utilized to create 3D ceramic microstructures with a resolution of several micrometers using preceramic polymers or ceramic-powder mixed polymers (Kawata et al., 2001). At this point, stereolithography via two-photon absorption polymerization is a very interesting technique for fabricating 3D ceramic patterns. This section proposes a new chemical approach for the fabrication of SiC ceramic microstructures with near-zero shrinkage from a new photosensitive precursor system using bifunctional inorganic polymer allylhydridopolycarbosilane (AHPCS) incorporated with organometallic (cyclopentadienylmethyl)-trimethylplatinum ($CpPtMe_3$) as a versatile additive. AHPCS is a well known precursor forstoichiometric SiC ceramics (Park etal., 2004), and $CpPtMe_3$ plays a versatile triple role as a photo-hydrosilylation catalyst upon 365 nm UV irradiation, a thermal hydrosilylation catalyst at elevated temperatures, and a two-photon absorbing initiator when exposed to a 710–800 nm laser (Boardman, 1992, Coenjarts & Ober, 2004). Therefore, it is expected that a simple AHPCS–CpPtMe3 mixture would form elaborate

dense networks via multiple curing routes between bifunctional groups, Si–H and the allyl group of the AHPCS, in sequential or/and coincidental reactions, which would result in little shrinkage with high ceramic yield during pyrolysis.

2D nanoscale line patterns were attempted with AHPCS mixed with 1 wt% of $CpPtMe_3$ (designated AHPCS–Pt) using a stereolithography process as an alternative terminology for the two-photon absorption fabrication technique. The AHPCS–Pt mixture was consolidated selectively using a laser beam with 780 nm wavelength for stereolithography, while AHPCS alone was not photocured. The patterned line width could be tailored by controlling the laser power and exposure time. The smallest line width of 320 nm was achieved at a laser power of 150 mW for a duration of 1 ms, which is a slightly lower resolution than the 210 nm reported previously for the acrylated polysilazane photoresist(Tuan et al., 2006).

Figure 9 shows various 3D SiC functional microstructures with dimensions of 1–5 μm obtained by pyrolysis at 600 °C in a nitrogen atmosphere from the AHPCS–Pt preceramic polymer features fabricated by a two-photon cross-linking process. There was no distortion or fracture of the structures, which often occurs through severe shrinkage. In contrast AHPCS alone or AHPCS mixed with two-photon absorbing (TPA) dyes could not form even 3D polymeric microstructures.

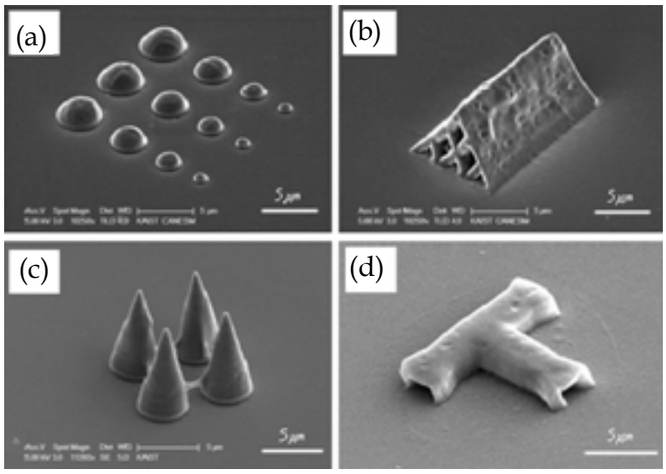

Fig. 9. Three-dimensional SiC ceramic microstructures obtained from pyrolysis at 600 1C of the AHPCS–Pt polymeric structure fabricated by stereolithography: (a) multi-scale hemispheres; (b) microchannel with multi-holes; (c) cones and (d) microscale multichannel

In the mushroom-shaped bolt shown in figure 10, the pyrolysed ceramic product (d,e) showed an 8.15 μm head dimension while the polymer structure (b,c) had a head size of 8.4 μm, as shown in figure 10(a). This clearly shows only 3% shrinkage in the top lateral direction during pyrolysis.

In order to confirm the extremely low shrinkage behaviour, spin-coated films on a Si wafer were prepared from AHPCS–Pt and AHPCS samples by UV exposure at 365 nm, post-curing at 160 °C, and pyrolysis at 600 °C. The effect of the $CpPtMe_3$ catalyst on the pyrolytic shrinkage was determined by comparing the behaviour of the AHPCS–Pt film with that of the alternative AHPCS film. The AHPCS–Pt derived ceramic film exhibited only 3% shrinkage; the thickness changed from 1.69 μm for the cured polymer to 1.64 μm after pyrolysis at 600 °C. On the other hand, AHPCS in the absence of a Pt additive exhibited 12% shrinkage with a change in film thickness from 1.32 μm to 1.16 μm. This is morphological

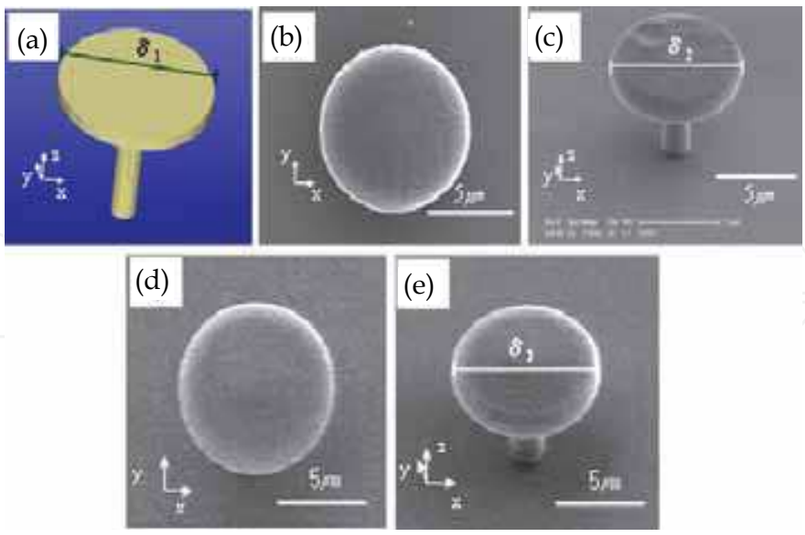

Fig. 10. Mushroom head bolt shape of SiC structure; (a) schematically designed structure (δ_1 = 8.4μm) and (b) top view of polymer state, (c) inclined view of the polymer state (δ_2 = 8.4 μm), (d) top view of the ceramic state, and (e) inclined view of the ceramic state (δ_3 = 8.15 μm).

evidence of the lower shrinkage of the AHPCS–Pt system during conversion from the polymer to ceramic phase, presumably due to the effective curing chemistry in the presence of a versatile $CpPtMe_3$ additive. In addition, the SiC film obtained from AHPCS without the Pt additive showed 12% shrinkage, which is significantly lower than the 40% in the case of SiCN from polyvinylsilazan being used as a precursor. This means that the AHPCS precursor also makes a significant contribution to decreasing the level of structural shrinkage.

4.2 Three-dimensional SiCN ceramic microstructures via nano-stereolithography of inorganic polymer photoresist

In this section, it is reported that a newly synthesized photosensitive preceramic polymer, a negative type of inorganic photoresist resin, is a suitable candidate for the fabrication of complex 3D sub-micrometer-sized structures via a two-photon absorbed crosslinking process followed by pyrolysis to form a ceramic phase which had been explained in previous section. The two-photon process including polymerization or/and crosslinking is recognized to be a promising technique for the fabrication of real 3D microstructures with a sub-micron resolution. This is shown for organic-based materials such as urethane acrylate, SU-8, and PDMS (Seet et al., 2005, Coenjarts & Ober, 2004). On the other hand, it is believed that an inorganic polymer photoresist is a promising material that could pave the way for a near-direct ceramic structuring process. In this work, a two-photon curable inorganic polymer (by mixing two-photon chromophore into a matrix of photosensitive inorganic polymer) was developed for the fabrication of 3D ceramic patterns.

In this work, the fabrication of two-dimensional (2D) and real three-dimensional (3D) nanoscale SiCN ceramic structures was attempted by a nano-stereolithography (NSL) process with a resolution of less than the diffraction limit, which can be difficult to obtain

using the conventional photolithographic technologies. The developed inorganic polymer photoresist containing 0.4 wt% of [1,4-bis(2-ethylhexyloxy)-2,5-bis(2-(4-(bis(4-bromophenyl)amino))-vinyl)benzene] (EA4BPA-VB) photosensitizer was selectively consolidated via a two-photon absorbed photocross-linking route, while the initial polyvinylsilazane was not photocuable. It is generally known that voxels, i.e. unit-volume-pixels, were controlled by altering the processing parameters of the NSL such as exposure time, laser power, and truncation amount of voxels under the substrates. As shown in figure 11 (a), the patterned line width can be tailored easily by controlling the laser power and the exposure time. The smallest line width of 210 nm was achieved under the conditions of a laser power of 100 mW and duration of 1 ms, whose resolution is comparable to the cases of reported two-photon materials. Moreover, the diameter and length of an elliptical voxel were both steeply broadened with the increase of laser power and exposure time close to the field of threshold energy for crosslinking. It was also determined from the experimental results that the higher power and longer exposure time enabled the fabrication of thick patterns.

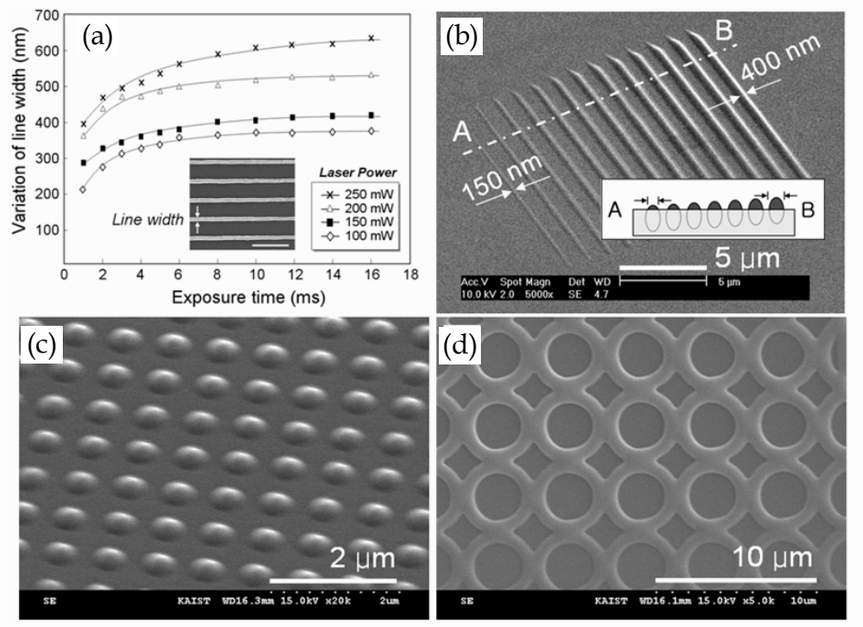

Fig. 11. (a) The dependence of line width at polymeric phase on laser power and exposure time as processing parameter study of nano-stereolithography. The inset shows an example of fabricated lines, and the scale bar is 2 μm. (b) to (d) show two-dimensional ceramic patterns pyrolyzed at 600°C; (b) multi-layered line patterns (c) ceramic nano-dots array with diameter 530 nm and (d) circle pattern.

Various 2D ceramic micropatterns were also fabricated by NSL and subsequent pyrolysis at 600°C (figure 11(b)~11(d)). Figure 11(b) shows line patterns fabricated by moving the beam focal position from the left-end to the right-end with 30 nm per line. It indicates that the line width can be controlled by the truncation amount under the glass plate, as illustrated in the inset of figure 11(b); actually reduced to 150 nm, that is lower than the minimum voxel

diameter. Alternative 2D ceramic patterns such as nano-dot array with 530 nm diameter and circle patterns were fabricated by adapting the aforementioned process parameters (figure 11(c) and 11(d)). Here, it is noteworthy to point out that the obtained ceramic patterns are useful as a tribological ceramic stamp (mold) with a nanoscale resolution suitable for various lithographic techniques such as hot embossing process, which is not achievable through conventional molds.

Eventually, the fabrication of a real 3D ceramic woodpile structure was performed by piling up the line patterns by layer-by-layer technique. The rectangular shape with a 9μm x 9μm x 9μm dimension was designed as shown by the schematic diagram in figure 12(a). However, after pyrolysis at 600°C, the photocured woodpile structure (figure 12(b)) was significantly deformed into a pyramid-like structure that nonlinearly tapered in a perpendicular direction (figure 12(c)). The lateral length of the top surface (W_T) was reduced to 5.3 μm with no change of bottom surface length (W_B). A dimensional change with a 41% shrinkage in the top lateral direction during pyrolysis occurred anisotropically with a different extent of shrinkage along the normal direction to the substrate. It can be interpreted that the bottom section adhered strongly to the glass substrate and was pyrolyzed under the constraint conditions, while the top section has a nearly free-standing condition. Here, it is generally reported that linear shrinkage in the range of 20~30% intrinsically occurs due to the thermal conversion from low dense polymer to a highly dense ceramic phase, accompanied with the weight loss. However, it is much less severe than in the case of sol-gel process, thus the preceramic polymers have been widely utilized via thermal curing and pyrolysis steps in a variety of high temperature material applications such as fibers and composites. (Liu et al., 2002)

The observed anisotropic shrinkage behavior must be a severe detrimental factor for a precise fabrication of 3D ceramic microstructures. In an attempt to rectify this shrinkage problem, silica particles with approximately 10 nm of diameter was introduced as filler into the inorganic photoresist resin with various solid loading portions. It was observed that the polymer-nanoparticle mixtures were kept transparent against laser beam due to homogeneous dispersion. When the identical structuring process and subsequent pyrolysis were conducted, the total amount of shrinkage in the lateral direction was considerably reduced to 33%, 28%, and 24% in each case of 20 wt%, 30 wt%, and 40 wt% silica particle loading samples, respectively (figure 12(d), 12(e), and 12(f)). Interestingly, through this, it was verified that the shrinkage can be reduced with a linear relation of 41(1-x)% for the silica particle percentage (x). In addition, the ceramic structure containing 40 wt% silica particle exhibited relatively isotropic shrinkage owing to its sliding free from the substrate during pyrolysis, presumably due to its weak interfacial adhesion to the substrate. Furthermore, other ceramic examples for real 3D structures of the spiral micro tube and cruciform were also fabricated with the developed resin polymer mixed with 40 wt% silica particles (figure 12(g) and 12(h)), suggesting novel applicability for chemical channels, or even for use in mechanical devices. The both structures with 90° twisting angles were originally designed with a side length 7.6 μm squared. After pyrolysis, the nearly isotropic shrinkage has occurred as the side lengths at the top and the bottom showed smaller discrepancy, with 5.81 μm and 6.23 μm in figure 12(g), 5.75 μm and 6.39 μm in figure 12(h), in contrast to these parameters of the non-free-standing structures. Here, it is believed that

the pyrolytic shrinkage can be improved by controlling the resin compositions as well as the geometric constraints, including the design of the compensated structure, with a prediction model simulation.

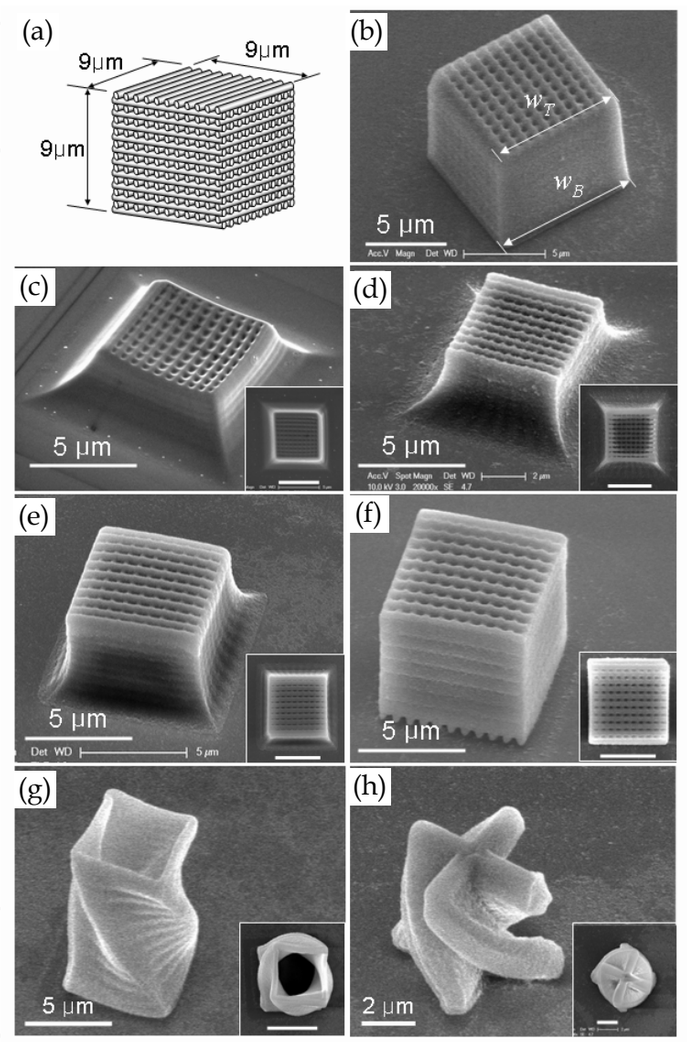

Fig. 12. Three-dimensional ceramic microstructures fabricated by nano-stereolithography or/and subsequent pyrolysis at 600°C; (a) schematically designed woodpile structure, (b) polymeric structure with no filler and (c) ceramic woodpile structure with no filler. Ceramic woodpile structure obtained from the mixed resin containing various amount of silica filler for reduced shrinkage; (d) 20 wt% silica, (e) 30 wt%, and (f) 40 wt%. Other 3D ceramic microstructures of spiral; (g) microtube and (h) microcruciform with twisting angle of 90° between their bottom and top; they are fabricated using the 40 wt% particle containing resin (each insert is top-views of the structure.).

5. Extended applications in the future

There are many possibilities for the adoption of micro ceramics structures in the fields of micro-reactors, diagnosis and sensors (e.g. microfludics, protein patterning and 3D ceramic structuring). For example, a microfluidic laboratory-on-a-chip have a wide variety of applications in liquid handling in biology and chemistry due to their ability to manipulate small sample quantities for rapid, high-resolution and low-cost analysis and synthesis (Guo et al., 2004, Sun & Kawata et al., 2004, Takada etal., 2005). Currently, microfluidics is mainly fabricated using polydimethylsiloxane (PDMS) and other organic polymers, owing to the flexibility and easy handling of the manufacturing microstructure. However, the general properties of organic polymers are not suitable for devices applicable to harsh environments requiring a high temperature tolerance, corrosion resistance and tribological properties. Therefore, there is a demand for the development of a process fabricating ceramic structures on the micro- or nano-scale. However, mechanical machining techniques in the fabricating the silicon, glass and metal microstructures have disadvantages such the requirement of high cost processing equipment as well as the limited resolution and geometry. It is believed that the integration of ceramic polymers into new economic manufacturing strategies can provide a break-through technology for the creation of complex ceramic microstructures with a nanoscale resolution. In addition, shrinkage control during pyrolysis is a critical issue in most applications of polymer-derived ceramics, which have been in strong demand for the development of an appropriate process for achieving the high dimensional stability of the final ceramic products.

6. Conclusion

Processes for fabricating the ceramic microstructures formed with SiC, SiCN and SiCBN, are in demand for use in areas such as microfluidics and MEMS that can be tolerated in harsh environments requiring a high temperatures tolerance, corrosion resistance, as well as tribological properties. This chapter describes the manufacturing techniques of SiC-based ceramic microstructrues by applying preceramic polymers with various fabrication techniques and subsequent pyrolysis to convert into ceramic phase. Firstly, macroporous and mesoporous SiC ceramic structures have been fabricated using various templates including packed silica sphere assemblies, porous carbon templates, and nanoporous silica structures. In addition, SiC nanotubes have also been obtained from an alumina membrane used as a template. These porous structures were generally obtained using a series of infiltration, curing and pyrolysis, and chemical or oxidative etching steps. Moreover, the feasible application of the microporous structures was attempted for high temperature ceramic microreactor to perform the on-demand reforming of higher hydrocarbons into hydrogen in portable power sources. Secondly, complex 3 dimensional SiC-based ceramic microfeatures were fabricated using near-net shape lithographic techniques with preceramic polymers. Line patterns and porous channels were produced by soft lithography, whereas the 3D woodpile structures were fabricated using stereolithography. These novel structures show great promises for future applications in tribological ceramic devices. It is expected that the integration of preceramic polymers into new economic manufacturing strategies such as precursor casting in templates and lithography utilization will be a break-through technology for the creation of complex ceramic nanostructures.

7. References

Boardman, L. D. (1992). *Organometallics*, Vol. 11, (4194-4201), 1099-0739

Caruso, F.; Shi, X. Y.; Caruso, R. A. & Susha, A. (2001). *Adv. Mater.*, Vol. 13, (740-744), 0935-9648

Chou, S.Y.; Krauss, P.R. & Renstrom, P. J. (1995). *Appl. Phys. Lett.*, Vol. 67, (3114-3116), 0034-6748

Coenjarts, C. A. & Ober, C. K. (2004). *Chem. Mater.* Vol. 16, (5556-5558), 0897-4756

Dai, H.; Wang, E. W.; Lu, Y. Z.; Fan, S.S. & Lieber, C. M. (1995). *Nature*, Vol. 375, (769-772), 0028-0836

Dibandjo, P.; Bois, L.; Chassagneux, F; Cornu, D.; Letoffe, J. M.; Toury, B.; Babonneau, F. & Miele, P. (2005). *Adv. Mat.*, Vol. 17, (571-574), 0935-9648

Donzel, C.; Geissler, M.; Berard, A.; Wolf, H.; Michel, B.; Hilborn, J. & Delamarche, E. (2001). *Adv. Mat.*, Vol. 13, (1164-1167), 0935-9648

Geis, S.; Fricke, J. & Löbmann, P. (2002). *J Eur. Ceram. Soc.*, Vol. 22, 1155-1161, 0955-2219

Guo, L. J.; Cheng, X. & Chou, C. F. (2004). *Nano Lett.*, Vol. 4, 69-73, 1530-6992

Heule, M. & Gauckler, L. J. (2001). *Adv. Mat.*, Vol. 13, (1790-1793), 0935-9648 , (2003). *Sensor Actuat. B*, Vol. 93, (100-106), 0935-9648

Heule, M.; Vuillemin, S. & Gauckler, L.J. (2003). *Adv. Mat.*, Vol. 15, (1237-1245), 0935-9648

Hong, L. Y. & Kim, D. P. (2005). *Key Eng. Mat.* Vol. 287, (323-328), 1013-9826

Iijima, S. (1991). *Nature*, Vol. 354, (56-58), 0028-0836

Lee, K. C. ; Seung S. & Lee, S. S. (2004). *Sens. Act. A*, Vol. 111, (37-43), 0924-4247

Liew, L.; Zhang, W.; Bright, V. M.; An, L.; Dunn, M. L. & Raj, R. (2001). *Sensor Actuat. A*, Vol. 89, (64-70), 0924-4247

Liew L.; Liu, Y.; Luo, R.; Cross, T.; An, L.; Bright, V. M.; Dunn, M. L.; Daily, J. W. & Raj, R. (2002). *Sensor Actuat. A*, Vol. 95, (120-134), 0924-4247

Liew, L. ; Bright, V. M. & Raj, R. (2003). *Sensor Actuat. A*, Vol. 104, (246-262), 0924-4247

Liu, Y.; Liew, L. A.; Liu, Y.; Luo, R.; An, L.; Dunn, M. L.; Bright, V. M.; Daily, J. W. & Raj, R. (2002). *Sensor. Actuat. A*. Vol. 95, (143-151), 0924-4247

Madou, M. J. (2002). *Fundamentals of Microfabrication - The Science of Miniaturization, 2nd ed.*, pp. 519-521, 978-0849308260, CRC Press, Boca Raton

Martin, C. R. & Aksay, I. A. (2005). *J Mater. Res.*, Vol. 20, (1995-2003), 0884-2914

Nguyen, N. T. & Wereley, S. T. (2002). *Fundamentals and Applications of Microfluidics*, pp. 82-97, 978-0-387-25564-4, Artech House, Boston

Kawata, S.; Sun, H. B.; Tanaka, T & Takada, K. (2001). *Nature*, Vol. 412, (697-698), 0028-0836

Keller, N.; Pham-Huu, C.; Ehret, G.; Keller, V. & Ledoux, M. J. (2003). *Carbon*, Vol. 41, (2132-2139), 0008-6223

Kim, E., Xia, Y. & Whitesides, G. M. (1996). *J Am. Chem. Soc.*, Vol. 118, (5722-5731), 0002-7863

Krawiec, P.; Weidenthaler, C. & Kaskel, S. (2004). *Chem. Mater.* Vol. 16, (2869-2880), 0959-9428

Kwon, S.; Son, G.; Suh, J. & Kim, K. T. (1994). *J Am. Ceram. Soc.*, Vol. 77, (3137-3141), 0002-7863

Parmentier, J.; Patarin, J.; Dentzer, J. & Vix-Guterl, C. (2002). *Ceram. Inter.*, Vol. 28, (1-7), 0272-8842

Park, K. H.; Sung, I. K. & Kim. D. P. (2004). *J Mater. Chem.*, Vol. 14, (1-4), 0959-9428
Park, K. H.; Sung, I. K. & Kim, D. P. (2004). *J Mater. Chem.* Vol. 14, (3436-3439), 0959-9428
Peng, H. X.; Fan, Z.; Evans, J. R. G. & Busfield, J. J. C. (2000). *J Eur. Ceram. Soc*. Vol. 20, (807-813), 0955-2219
Pham, T. A.; Lim, T. W.; Park, S. H.; Yang D. Y. & Kim, D. P. (2006). *Adv. Funct. Mater.*, Vol. 16, (1235-1241), 1616-301X
Pham-Huu, C.; Bouchy, C.; Dintzer, T.; Ehret, G.; Estournes, M. & Ledoux, M. J. (1999). *Appl. Catal. A*, Vol. 180, (385-397), 0926-860X
Qin, D.; Xia, Y.; Rogers, J. A.; Jackman, R. J.; Zhao, X. M. & Whitesides, G. M. (1999). *Microsystem Technology in Chemistry and Life Science*, Ed. by Manz, A. and Becker, H., pp. 1-20, 10: 354063424X, Springer, Berlin
Quin, J.; Wang, J.; Zhihao, J. & Qiao, G. (2003). *Mat. Sci. Eng. A*, Vol. 358, (304-309), 0965-0393
Schmidt-Winkel, P.; Lukens, W. W. Jr.; Zhao, D. Y.; Yang, P. D.; Chmelka, B. F. & Stucky, G. D. (1999). *J Am. Chem. Soc*. Vol. 121, (254-255), 0002-7863
Seet, K. K.; Mizeikis, V.; Matsuo, S.; Juodkazis, S. & Misawa, H. (2005). *Adv. Mater*. Vol. 17, (541-545), 0935-9648
Sepulveda, P. (1997). *Am. Ceram. Soc. Bull*, Vol. 76, (61-65), 1226-086X
Shah, S. R. & Raj, R., J. (2005). *J Eur Ceramic Soc.*, Vol. 25, (243-249), 0955-2219
Shi, Y. F.; Meng, Y.; Chen, D. H.; Cheng, S. J.; Chen, P.; Yang, H. F.; Wan, Y. & Zhao, D. Y. (2006). *Adv. Funct. Mater.*, Vol. 16, (561-567), 1616-301X
Sun, H. B. & Kawata, S. (2004) *Adv. Polym. Sci.*, Vol. 170, (169-273), 0065-3195
Sung, I. K.; Yoon, S. B.; Yu, J. S. & Kim. D. P. (2002). *Chem. Comm.*, Vol. 2002, (1480-1481), 1359-7345
Takada, K.; Sun, H. B. & Kawata, S. (2005). *Appl. Phys. Lett.*, Vol. 86, (071122-1 - 071122-3, 0003-6951
Vinu, A.; Terrones, M.; Golberg, D.; Hishita, S.; Ariga, K. & Mori, T. (2005). *Chem. Mater.*, Vol. 17, (5887-5890), 0897-4756
Wang, H.; Yu, J. S.; Li, X. D. & Kim, D. P. (2004). *Chem. Comm.*, Vol. 2004, (2352-2353), 1359-7345
Wang, H.; Li, X. D.; Yu, J. S & Kim, D. P. (2004). *J Mat. Chem.*, Vol. 14, (1383-1386), 0959-9428
Wang, H.; Li, X. D. & Kim, D. P. (2005). *Appl. Organomet. Chem.* Vol. 19, (742-749), 0268-2605
Wang, H; Li, X. D.; Kim, T. S. & Kim, D. P. (2005). *Applied Phy. Lett.*, Vol. 86, (1-3), 0003-6951
Wang, H.; Zheng, S. Y.; Li, X. D. & Kim. D. P. (2005). *Micropor. Mesopor. Mat.*, Vol. 80, (357-362), 1387-1811
Wu, G.; Zhang, L.; Cheng, B.; Xie, T. & Yuan, X. (2004). *J Am. Chem. Soc.*, Vol. 126, (5976-5977), 0002-7863
Yamazaki, K. & Namatsu, H. (2004). *Microelectron. Eng.*, Vol. 73-74, (85-89), 0167-9317
Yan, J.; Wang, A. & Kim. D. P. (2006). *J Phys. Chem. B*, Vol. 110, (5429-5433), 1089-5647
Xia, Y. & Whitesides, G. M. (1998). *Annu. Rev. Mater. Sci.*, Vol. 28, (153-184), 1225-0112
Xia, Y.; Rogers, J. A.; Paul, K. E. & Whitesides, G. M., (1999). *Chem. Rev.*, Vol. 99, (1823-1848), 0009-2665
Zhang, F. Z.; Kato, T.; Fuji, M. & Takahashi M. (2006). *J Eur. Ceram. Soc.*, Vol. 26, (667-671), 0955-2219

Zhao, D. Y.; Feng, J. L.; Huo, Q. S.; Melosh, N.; Fredrickson, G. H.; Chmelka, B. F. & Stucky, G. D. (1998). *Science*, Vol. 279, (548-550), 0036-8075
Zhu, X.; Jiang, D. & Tan, S. (2002). *Mater. Res. Bull.*, Vol. 37, (541-553), 0025-5408

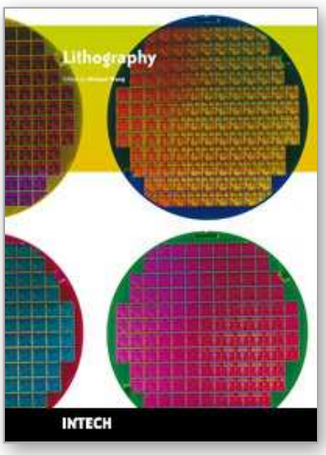

Lithography

Edited by Michael Wang

ISBN 978-953-307-064-3
Hard cover, 656 pages
Publisher InTech
Published online 01, February, 2010
Published in print edition February, 2010

Lithography, the fundamental fabrication process of semiconductor devices, plays a critical role in micro- and nano-fabrications and the revolution in high density integrated circuits. This book is the result of inspirations and contributions from many researchers worldwide. Although the inclusion of the book chapters may not be a complete representation of all lithographic arts, it does represent a good collection of contributions in this field. We hope readers will enjoy reading the book as much as we have enjoyed bringing it together. We would like to thank all contributors and authors of this book.

How to reference

In order to correctly reference this scholarly work, feel free to copy and paste the following:

Tae-Ho Yoon, Lan-Young Hong and Dong-Pyo Kim (2010). Fabrication of SiC-based Ceramic Microstructures from Preceramic Polymers with Sacrificial Templates and Softlithography Techniques, Lithography, Michael Wang (Ed.), ISBN: 978-953-307-064-3, InTech, Available from: http://www.intechopen.com/books/lithography/fabrication-of-sic-based-ceramic-microstructures-from-preceramic-polymers-with-sacrificial-templates

INTECH
open science | open minds

InTech Europe
University Campus STeP Ri
Slavka Krautzeka 83/A
51000 Rijeka, Croatia
Phone: +385 (51) 770 447
Fax: +385 (51) 686 166
www.intechopen.com

InTech China
Unit 405, Office Block, Hotel Equatorial Shanghai
No.65, Yan An Road (West), Shanghai, 200040, China
中国上海市延安西路65号上海国际贵都大饭店办公楼405单元
Phone: +86-21-62489820
Fax: +86-21-62489821

IntechOpen